Bioorganic & Medicinal Chemistry 19 (2011) 5776–5781

Contents lists available at SciVerse ScienceDirect

Bioorganic & Medicinal Chemistry

journal homepage: www.elsevier.com/locate/bmc

Potential AMPK activators of cucurbitane triterpenoids from *Siraitia grosvenorii* Swingle

Xu-bing Chen [a,†], Jing-jing Zhuang [a,†], Jun-hua Liu [a], Min Lei [b], Lei Ma [a], Jing Chen [b,*], Xu Shen [a,b], Li-hong Hu [a,b,*]

[a] School of Pharmacy, East China University of Science and Technology, 130 Meilong Road, Shanghai 200237, China
[b] Shanghai Research Center for Modernization of Traditional Chinese Medicine, Shanghai Institute of Materia Medica, Chinese Academy of Sciences, Shanghai 201203, China

ARTICLE INFO

Article history:
Received 17 June 2011
Revised 12 August 2011
Accepted 12 August 2011
Available online 22 August 2011

Keywords:
Siraitia grosvenorii Swingle
Cucurbitane triterpenoids
AMPK
HepG2 cell
Anti-diabetic effect

ABSTRACT

AMP-activated kinase (AMPK) as a key controller in the regulation of whole-body energy homeostasis, plays an important role in protecting the body from metabolic diseases. Recently, improved glucose, lipid utility and increased insulin sensitivity were observed on several diabetic rodent models treated with crude mogrosides isolated from the fruit of *Siraitia grosvenorii* Swingle, but the precise active compounds responsible for the anti-diabetic activity of this plant have not been clearly identified. In our current work, acid hydrolysis of crude mogrosides provided five new cucurbitane triterpenoids (**1**–**4**, **8**), along with three known ones (**5**–**7**). The main aglycone mogrol (**7**) and compounds **4** and **8** were found to be potent AMPK activators in the HepG2 cell line. This result suggested AMPK activation by the mogroside aglycones **7** and **8** was proved to contribute at least partially to the anti-hyperglycemic and anti-lipidemic properties in vivo of *S. grosvenorii*.

1. Introduction

Metabolic disorders, including obesity and type-2 diabetes, are now taking its place as one of the main threats to human health in 21st century.[1] Imbalance of energy metabolism is a major cause for metabolic syndrome.[2,3] Recently, many studies suggested that AMP-activated protein kinase (AMPK), a heterotrimetric protein, plays a key role in regulation of whole-body energy homeostasis. AMPK is activated under a variety of conditions that signify cellular stress and usually reflected by a change in the intracellular ATP-to-AMP ratio. Active AMPK orchestrates a variety of metabolic processes, most of which lead to reduced energy storage and increased energy production. Therefore, the activation of AMPK is considered as a potential therapeutic target for the treatment of metabolic disorders.[4]

Luo Han Guo is the fruit of *Siraitia grosvenorii* Swingle (formerly called *Momordica grosvenorii* Swingle) belonging to Cucurbitaceae species and is used as a pulmonary demulcent and emollient for the treatment of dry cough, sore throat, dire thirst, and constipation in traditional Chinese medicine.[5] The main chemical components of the fruit of this plant are cucurbitane triterpene glycosides, known as mogrosides, which have high sweetness, low calories, and can serve as a substitute for sugar for obese and diabetic patients.[6,7] Recently, improved glucose and lipid utility and increased insulin sensitivity were observed on several diabetic rodent models treated with crude mogrosides by oral administration, for example, diet-induced obese mice,[8] Goto–Kakizaki rats[9] and alloxan-induced diabetic mice.[10–12] Although several mechanisms were proposed to explain the anti-hyperglycemic effects of crude mogrosides, such as crude mogrosides are α-glucosidase inhibitors,[13] and crude mogrosides and mogroside V, the main chemical component of crude mogrosides, function as insulin secretagogues.[14] However, Murata et al.[15] reported mogroside V was mostly degraded by digestive enzymes and intestinal microflora, and its aglycone, mogrol, was found in the portal blood. Therefore, the precise active compounds responsible for the anti-diabetic activity of this plant have not been clearly identified and their related mechanisms of anti-diabetic effects should be further investigated.

Recently, anti-diabetic activities of cucurbitane triterpenoids isolated from bitter melon (Cucurbitaceae) were reported and associated with activation of the AMPK pathway.[16] Since their contents in bitter melon were only about 3 ppm, the further study of cucurbitane triterpenoids in anti-diabetic drug development were limited. So it is necessary to explore the new resources of cucurbitane triterpenoids.

In this work, we investigated the chemical constituents of crude mogrosides by acid hydrolysis for the purpose of identifying the

* Corresponding authors. Tel.: +86 21 50806600x2118; fax: +86 21 50806031 (J.C.); tel.: +86 21 20231965; fax: +86 21 20231965 (L.-h.H.).
E-mail addresses: jingchen@mail.shcnc.ac.cn (J. Chen), simmhulh@mail.shcnc.cn (L.-h. Hu).
† These authors contributed equally to this work.

0968-0896/$ - see front matter © 2011 Elsevier Ltd. All rights reserved.
doi:10.1016/j.bmc.2011.08.030

anti-diabetic principles of this medicinal herb. We have isolated five new cucurbitane triterpenoids (**1**–**4**, **8**, Fig. 1), along with three known ones (**5**–**7**, Fig. 1), and found the mogroside aglycones **7** and **8** are potent AMPK activators in HepG2 cells, which might be a cause to result in the anti-diabetic effect of crude mogrosides.

2. Results and discussion

2.1. Structural determination of compounds 1–9

Repeated column chromatography of the acid-hydrolysis product of crude mogrosides resulted in the isolation of compounds (**1**–**8**). Three known compounds were identified as bryogenin (**5**),[17] bryodulcosigenin (**6**),[17,18] and mogrol (**7**)[6,17] by comparison of the spectroscopic data with reported data. The main component mogroside V (**9**)[17,19] was directly isolated from the crude mogrosides.

Compound **1** was obtained as a white amorphous powder. Its molecular formula was determined as $C_{31}H_{52}O_4$ by HRESIMS at *m/z* 511.3754 $[M+Na]^+$ (calcd for 511.3763). The IR spectrum of 1 showed absorption bands at 3446 (hydroxyls) and 1693 (carbonyl) cm^{-1}. The ^1H NMR spectrum data (Table 1) showed the presence of eight methyl groups at δ_H 0.74, 1.01, 1.02, 1.08, 1.11, 1.11, 1.16 (each 3H, s), and 0.87 (3H, d), one methoxyl at δ_H 3.22 (3H, s). Further features were observed at δ_H 3.39 (1H, d, J = 9.5 Hz), at δ_H 3.47 (1H, br s), and at δ_H 5.65 (1H, d, J = 5.9 Hz, a vinylic proton). The ^{13}C NMR spectrum data of **1** (Table 1) revealed the signals of one carbonyl group (δ_C 214.9), one olefin group (δ_C 139.4, 120.6), two oxygenated CH groups (δ_C 76.1, 76.8), and one oxygenated C group (δ_C 77.5). Detailed comparison of the NMR data of **1** with those of bryodulcosigenin (**6**)[17,18] suggested that compound **1** was very similar to bryodulcosigenin, except that compound **1** contains one OCH_3 group more than bryodulcosigenin. The location of the additional OCH_3 group (C-25) was assigned by HMBC correlations of H-31 to C-25 and those of H-26, H-27 to C-31. Therefore, the structure of **1** was established as 25-methoxy-11-oxomogrol.

Compound **2** was isolated as a white amorphous powder. Its molecular formula was established as $C_{31}H_{54}O_4$ by HRESIMS at *m/z* 513.3911 $[M+Na]^+$ (calcd for 513.3920). The NMR spectra (Table 1) were very similar to those of mogrol (**7**),[6,17] except that compound **2** contains one OCH_3 group more than mogrol. The location of the additional OCH_3 group (C-25) was assigned by HMBC correlations H-31 to C-25 and H-26, H-27 to C-31. Thus, the structure of **2** was identified as 25-methoxymogrol.

Compound **3** was obtained as a white amorphous powder. The IR spectrum of **3** exhibited absorptions of one carbonyl (1706 cm^{-1}) and hydroxyl groups (3444 cm^{-1}). The molecular formula of **3** was determined to be $C_{30}H_{50}O_3$ by HRESIMS at *m/z* 459.3832 $[M+H]^+$ (calcd for 459.3838), corresponding to the presence of 6° of unsaturation. The NMR data of **3** revealed the signals of one carbonyl group (δ_C 214.9), one olefin group [δ_H 5.54 (1H, d, J = 6.2 Hz), δ_C 142.1, 121.3)], two oxygenated CH groups [δ_H 3.41 (1H, br s), 3.89 (1H, m), δ_C 76.6, 77.6)], and eight methyl groups [δ_H 0.79 (3H, s), 0.84 (3H, s), 1.03 (3H, s), 1.04 (3H, s), 1.07 (3H, s), 1.09 (3H, s), 1.11 (3H, s), 0.87 (3H, d, J = 6.4)]. In comparison of the ^1H and ^{13}C NMR data of **3** with those of the mogrol (**7**),[6,17] they were very similar, except that compound **3** contains one carbonyl group more than mogrol and two hydroxyl groups (C-24 and C-25) less than mogrol. The HMBC correlations between H-25, H-26, H-27, and H-22 to C-24 (δ_C 215.7) implied that the carbonyl group was located at C-24. Therefore, Compound **3** was determined as 25-dehydroxy-24-oxomogrol.

The structure determination of Compound **4** was carried out on a similar manner to that described for **3**. Compound **4** was also obtained as a white amorphous powder. Its molecular formula was determined as $C_{30}H_{50}O_3$ by HRESIMS at *m/z* 481.3651 $[M+Na]^+$ (calcd for 481.3658). The IR spectrum of **4** Showed absorption bands at 3438 (hydroxyls) and 1704 (carbonyl) cm^{-1}. Compound

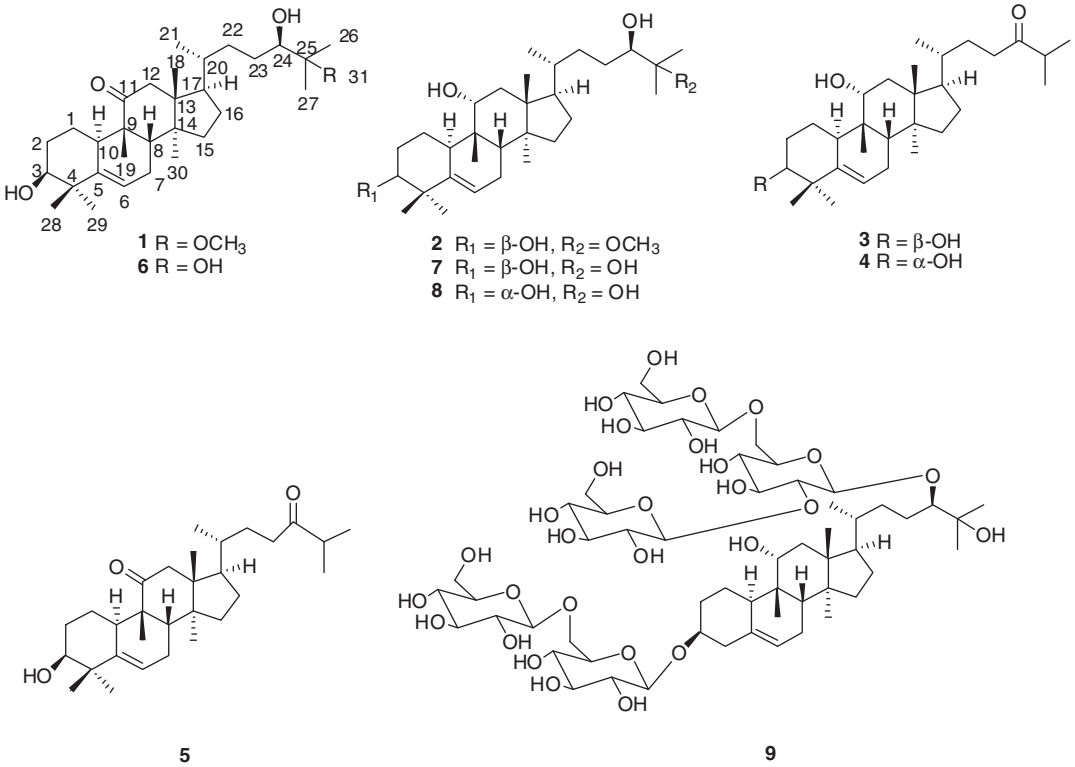

Figure 1. The structures of compounds **1**–**9**.

Table 1
NMR spectroscopic data for compounds **1–3** in $CDCl_3$

Pos.	1[a]		2[a]		3[b]	
	δ_H (J in Hz)	δ_C, mult.	δ_H (J in Hz)	δ_C, mult.	δ_H (J in Hz)	δ_C, mult.
1	1.40 br s	20.5, CH_2	1.37 m 1.28 m	27.9, CH_2	1.92 br s	28.1, CH_2
2	1.67 br s 1.77 br s	28.5, CH_2	1.61 m	29.1, CH_2	1.62 br s	29.3, CH_2
3	3.47 br s	76.1, CH	3.44 br s	76.4, CH	3.41 br s	76.6, CH
4		41.5, C		42.0, C		42.2, C
5		139.4, C		141.9, C		142.1, C
6	5.65 d (5.9)	120.6, CH	5.55 d (6.1)	121.0, CH	5.54 d (6.2)	121.3, CH
7	2.42 br s 1.92 br s	23.9, CH_2	2.38 m 1.80 br s	24.1, CH_2	2.34 m	24.3, CH_2
8	1.94 br s	43.7, CH	1.64 m	43.0, CH	1.65 br s	43.2, CH
9		48.7, C		39.7, C		39.9, C
10	1.43 br s	35.7, CH	2.25 m	35.7, CH	2.43 m	35.8, CH
11		214.9, C	3.91 t (8.5)	78.7, CH	3.89 m	79.0, CH
12	2.94 d (4.6) 2.46 br s	48.4, CH_2	1.82 br s	40.2, CH_2	1.73 br s	30.2, CH_2
13		49.1, C		47.1, C		47.4, C
14		48.7, C		49.0, C		49.5, C
15	1.35 br s	34.3, CH_2	1.17 br s 1.08 m	34.0, CH_2	1.28 m	34.2, CH_2
16	1.24 br s	29.7, CH_2	2.22 dd (13.3, 3.5)	25.4, CH_2	2.19 d (13.3)	25.6, CH_2
17	1.69 br s	49.6, CH	1.58 m	50.3, CH	1.60 br s	50.4, CH
18	0.74 s	16.7, CH_3	0.87 s	16.6, CH_3	0.84 s	16.9, CH_3
19	1.11 s	20.0, CH_3	1.11 s	25.7, CH_3	1.03 s	26.6, CH_3
20	2.31 m	35.3, CH	1.42 m	35.9, CH	1.76 br s	41.1, CH
21	0.88 d (6.3)	18.3, CH_3	0.91 d (6.3)	18.5, CH_3	0.87 d (6.4)	18.5, CH_3
22	1.48 m	27.8, CH_2	1.37 overlapped	27.9, CH_3 overlapped	2.30 m	37.6, CH_3
23	2.04 m 1.32 m	34.0, CH_2	1.44 m 1.26 m	33.2, CH_2	2.57 m	40.3, CH_2
24	3.39 d (9.5)	76.8, CH	3.39 d (9.6)	76.8, CH		215.7, C
25		77.5, C		77.5, C	1.54 br s	35.9, CH
26	1.08 s	18.6, CH_3	1.08 s	18.7, CH_3	1.07 s	18.6, CH_3
27	1.11 s	20.7, CH_3	1.11 s	20.7, CH_3	1.04 s	18.7, CH_3
28	1.02 s	27.3, CH_3	1.05 s	26.3, CH_3	1.09 s	26.0, CH_3
29	1.16 s	25.3, CH_3	1.13 s	25.7, CH_3	1.11 s	25.9, CH_3
30	1.01 s	18.2, CH_3	0.80 s	18.9, CH_3	0.79 s	19.2, CH_3
31	3.22 s	49.0, CH_3	3.21 s	49.3, CH_3		

[a] 400 MHz for ^1H and 100 MHz for ^{13}C.
[b] 300 MHz for ^1H and 75 MHz for ^{13}C.

4 and **3** not only had same molecular formula, but also had very similar NMR data. The subtle difference was that the peak of H-3 at δ_H 3.19 (dd, J = 11.5, 4.7 Hz) in **4** was shifted upfield compared with the H-3 signal at δ_H 3.41 (br s) in **3**. The 11.5 and 4.7 Hz of coupling constant of H-3 in **4** revealed that H-3 was β-oriented. Thus, the structure of compound **4** was determined as 3α-hydroxy-25-dehydroxy -24-oxomogrol.

Compound **8** was isolated as a white amorphous powder. Its molecular formula was determined as $C_{30}H_{52}O_4$ by HRESIMS at m/z 522.3911 $[M+COOH]^-$ (calcd for 522.3920). The IR spectrum of **4** showed absorption bands at 3431 (hydroxyls) cm^{-1}. Comparison of the NMR data of **8** with those of mogrol suggested that compound **8** was very similar to mogrol, except that the signal of H-3 at δ_H 3.40 (t, J = 2.7 Hz)[6] in mogrol was replaced by that of H-3 at δ_H 3.18 (dd, 11.4, 4.8) in **8**. The values of coupling constants (H-3) of compound **8** revealed that H-3 was β-oriented. Therefore, compound **8** was determined as 3α-hydroxymogrol.

By comparison the structures of cucurbitane triterpenoids **1–8** with those of all reported mogrosides, we doubted the compounds **1** and **2** with 25-methoxyl group and compounds **3**, **4**, and **5** with 24-carbonyl group are artifacts, which further confirmed by acid hydrolysis of compound **7** producing compounds **2** and **3**.

We propose a plausible mechanism for the formation of artificial compounds **2** and **3** from **7** at presence of HCl (Scheme 1). By treating with HCl, **7** firstly lose a water to form 25-carbocation intermediate (**10**), then to yield **3** by 1,2-shift of hydride and to **2** by being quenched with methanol.

2.2. Activation of AMPK by compounds 1–9 in HepG2 cells

The effects of compounds (**1–8**) and mogroside V (**9**) on AMPK phosphorylation were measured in HepG2 cells. In this assay, berberine acted as a positive control and exhibited the significant effect on AMPK phosphorylation increasing (Fig. 2A), which was consistent with the reported result.[20] As shown in Figure 2B–D, compounds **7** and **8** at 1, 10, 20 μM and compoumd **4** at 10 μM could increase AMPK phosphorylation more efficiently than berberine, while compounds **1**, **2**, **3**, **5**, and **6** had moderate effects on AMPK phosphorylation and the major ingredient mogroside V (**9**) of crude mogrosides had no effects. These results suggested AMPK activation by the mogroside aglycones 7 and 8 is proved to contribute at least partially to the anti-hyperglycemic and anti-lipidemic properties in vivo of *S. grosvenorii*.

Furthermore, compounds were prepared to establish structure–activity relationships for activation of AMPK phosphorylation. Comparison their activities between **2** and **7**, **3** and **4**, **3** and **7**, **6** and **7** suggested that 25-hydroxyl, 3α-hydroxyl, 24β-hydroxyl, 11α-hydroxyl substituents were more favorable to activate AMPK phosphorylation than 25-methoxyl, 3β-hydroxyl, 24-carbonyl, 11-carbonyl substituents, respectively. The total saponins content is about 24% from commercial crude mogrosides and the obtained yield of main active aglycone mogrol is about 3.14%, whereas their content in bitter melon is about 3 ppm. Therefore, mogrol is a better lead structure for development of new class of AMPK-activating agents.

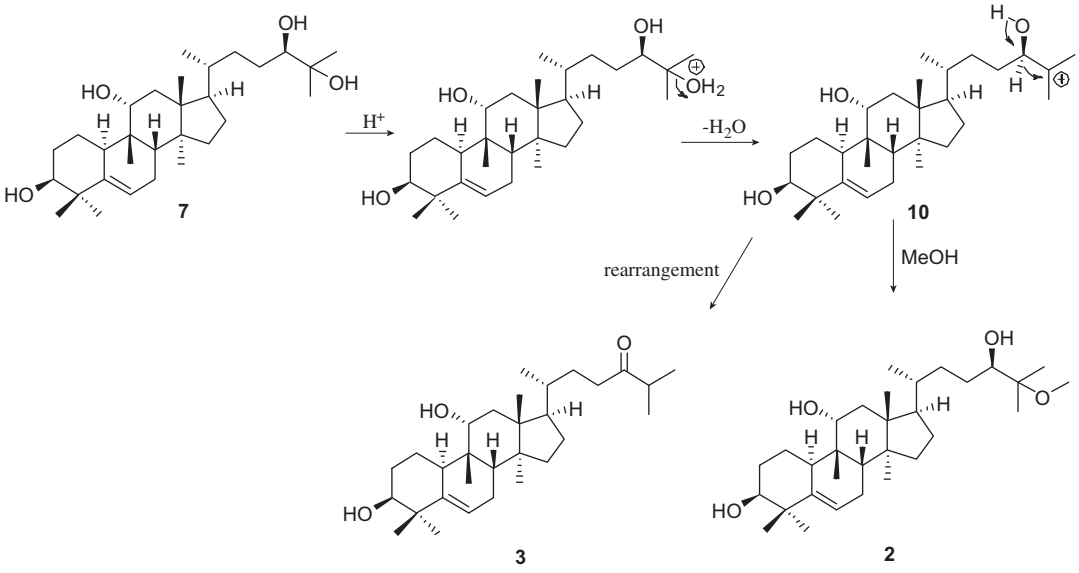

Scheme 1. Plausible mechanism for the formation of artifacts **2** and **3** from **7**.

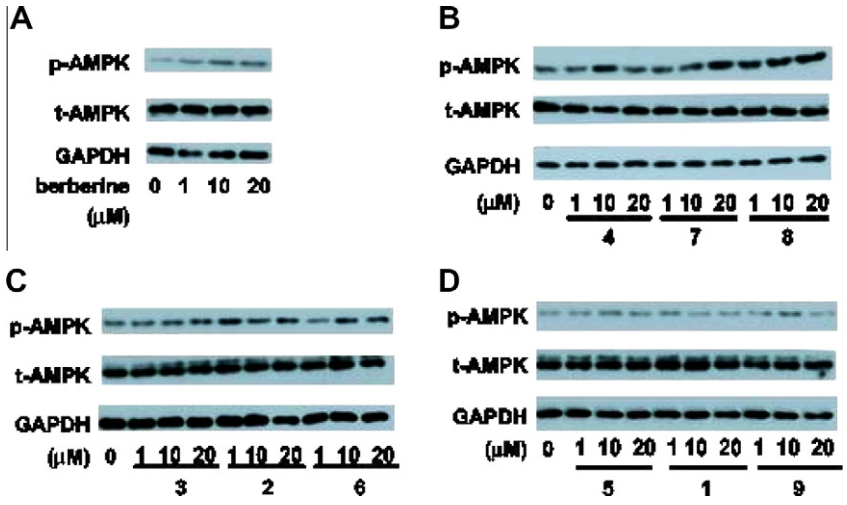

Figure 2. The effects of berberine and acid-hydrolysis products of crude mogrosides on AMPK phosphorylation in HepG2 cells. (A) The effects of berberine on AMPK phosphorylation. HepG2 cells were treated with indicated concentrations of berberine (1, 10, and 20 μM) for 30 min, AMPK phosphorylation level and total AMPK level were determined by western blotting. (B–D) The effects of acid-hydrolysis products of crude mogrosides on AMPK phosphorylation. HepG2 cells were treated with indicated concentrations of compounds (1, 10, and 20 μM) for 30 min, AMPK phosphorylation level and total AMPK level were determined by western blotting. The results shown are representative of three independent experiments. $^{*}p$ <0.05; $^{**}p$ <0.01; $^{***}p$ <0.005; one-way ANOVA.

3. Experimental section

3.1. General experimental procedures

Optical rotations were measured with a Shenke SGW-1 automatic polarimeter. IR spectra were measured in a Perkin-Elmer 341 spectrometer with KBr pellets. NMR spectra were obtained at 300 and 400 MHz in $CDCl_3$ using Varian Inova spectrometers. ESIMS were performed on an Waters Acquity SQD single-quadrupole mass spectrometer. HPLC analyses were performed on a Waters 2690 unit with Alltech 3300 evaporative light scattering detector, using a Kromacil C_{18} column (4.6 × 150 mm, 5 μm). Column chromatography was carried out on Silica gel (200–300 mesh) and TLC on GF254 silica gel plates (Yantai Huiyou Inc., China). Product isolation was performed with RP-18 (20–45 μm, Fuji Silysia Chemical Ltd, Japan) or sephadex LH-20 (20–100 μm, Pharmacia) or MCI Gel CHP20P (75–150 μm, Mitsubishi Kasei Chemical Industries).

3.2. Plant material

The crude mogrosides (production specification: total saponins content ⩾24%; production code 20100723) from *S. grosvenorii* Swingle was purchased from Huizhou Eastern Plant Health Technology Co. Ltd, in Guangdong Province, People's Republic of China, in September 2010.

3.3. Isolation procedure

The crude mogrosides (100 g) was suspended in 200 mL of MeOH and hydrolysed with 100 mL of 4 mol/L HCl at 80 °C for 2 h. The mixture was left to cool, diluted with H_2O, and filtered,

and the aqueous acid solution was neutralized with 1 N KOH and then concentrated. The residue was suspended in H_2O and partitioned with EtOAc. The EtOAc (29.6 g) fraction was subjected to silica gel column chromatography with a gradient elution system of CH_2Cl_2–MeOH (100:1–20:1) to obtain two fractions (A–B). Fraction A (8.0 g) was separated by silica gel column (CH_2Cl_2–MeOH, 60:1) to yield three fractions (A1–A3). Fraction A1 (2.3 g) was subjected to passage over a silica gel column with a gradient elution system of petroleum ether–ethyl acetate (6:1–4:1). Then the fractions were purified by sephadex LH-20 column chromatography (MeOH) to afford compounds **5** (95 mg), **1** (13 mg), and **3** (203 mg). Fraction A2 (1.5 g) was purified by silica gel column with a system of petroleum ether–ethyl acetate (4:1) to yield compound **4** (228 mg). Fraction A3 (2.1 g) was subjected to a silica gel column with a system of petroleum ether–ethyl acetate (2:1) and then RP-18 column (MeOH–H_2O, 80:20) to yield compounds **2** (14 mg) and **6** (752 mg). Fraction B (6.2 g) was separated by silica gel column (CH_2Cl_2–MeOH, 30:1) and then MCI Gel CHP20P (MeOH–H_2O, 80:20) to obtain compounds **7** (3.1 g) and **8** (488 mg). The crude mogrosides (8 g) was suspended in 20 mL of MeOH and filtered. After removal of the solvent by evaporation, the residue was separated by RP-18 column (MeOH–H_2O, 60:40, 70:30, respectively) to yield Compound **9** (257 mg).

3.3.1. 25-Methoxy-11-oxomogrol (1)

White powder; $[\alpha]_D^{20}$ + 182 (*c* 0.05, MeOH); IR (KBr) ν_{max} 3446 (OH), 2962, 2921, 2875, 1693 (CO), 1635, 1463, 1382, 1079, 977, 620 cm^{-1}; ^1H NMR and ^{13}C NMR, see Tables 1 and 2; ESIMS *m/z* 511.5 $[M+Na]^+$; HRESIMS *m/z* 511.3754 $[M+Na]^+$ (calcd for $C_{31}H_{52}O_4Na$, 511.3763).

3.3.2. 25-Methoxymogrol (2)

White powder; $[\alpha]_D^{20}$ + 48 (*c* 0.05, MeOH); IR (KBr) ν_{max} 3442 (OH), 3000, 2948, 1625, 1465, 1378, 1072, 559 cm^{-1}; ^1H NMR and ^{13}C NMR, see Tables 1 and 2; ESIMS *m/z* 513.6 $[M+Na]^+$; HRESIMS *m/z* 513.3911 $[M+Na]^+$ (calcd for $C_{31}H_{54}O_4Na$, 513.3920).

3.3.3. 25-Dehydroxy-24-oxomogrol (3)

White powder; $[\alpha]_D^{20}$ + 11 (*c* 0.15, MeOH); IR (KBr) ν_{max} 3444 (OH), 3000, 2958, 2873, 1706 (CO), 1635, 1465, 1378, 1074, 1025, 979, 408 cm^{-1}; ^1H NMR and ^{13}C NMR, see Tables 1 and 2; ESIMS *m/z* 459.5 $[M+H]^+$; HRESIMS *m/z* 459.3832 $[M+H]^+$ (calcd for $C_{30}H_{51}O_3$, 459.3838).

3.3.4. 3-Hydroxy-25-dehydroxy-24-oxomogrol (4)

White powder; $[\alpha]_D^{20}$ + 28 (*c* 0.05, MeOH); IR (KBr) ν_{max} 3438 (OH), 2962, 2938, 2875, 1704 (CO), 1633, 1467, 1380, 1022, 958 cm^{-1}; ^1H NMR and ^{13}C NMR, see Table 1 and 2; ESIMS *m/z* 481.4 $[M+Na]^+$; HRESIMS *m/z* 481.3651 $[M+Na]^+$ (calcd for $C_{30}H_{50}O_3Na$, 481.3658).

3.3.5. 3-Hydroxymogrol (8)

White powder; $[\alpha]_D^{20}$ + 58 (*c* 0.05, MeOH); IR (KBr) ν_{max} 3431 (OH), 2945, 1635, 1468, 1379, 1020, 958, 557 cm^{-1}; ^1H NMR and ^{13}C NMR, see Tables 1 and 2; ESIMS *m/z* 521.5 $[M+COOH]^-$; HRESIMS *m/z* 521.3837 $[M+COOH]^-$ (calcd for $C_{31}H_{53}O_6$, 521.3842).

3.4. Identification of compounds 2 and 3 as artifacts

Compound **7** (100 mg) was dissolved in methanol (3 mL), then 3 mL of 4 N HCl was added, and stirred for 2 h at 80 °C. The mixture was cooled and neutralized with 1 N KOH, then extracted with EtOAc. We further analyzed the EtOAc extract by LC–MS and detected the presence of compounds **2** and **3** by comparison their molecular weights and retention times with those of standard samples (see Supplementary data).

Table 2
NMR spectroscopic data for compounds **4** and **8** in $CDCl_3$

Pos.	4[a]		8[a]	
	δ_H (*J* in Hz)	δ_C, mult.	δ_H (*J* in Hz)	δ_C, mult.
1	1.82 m	29.9, CH_2	1.30 m	28.5, CH_2
2	1.62 br s	31.3, CH_2	1.74 m	31.4, CH_2
3	3.19 dd (11.5, 4.7)	79.0, CH	3.19 dd (11.5, 4.3)	77.7, CH
4		42.7, C		42.8, C
5		144.8, C		144.8, C
6	5.57 d (5.6)	118.8, CH	5.57 d (5.7)	118.7, CH
7	2.39 m	24.2, CH_2	2.34 m	24.3, CH_2
			1.83 m	
8	1.65 br s	43.1, CH	1.62 m	43.1, CH
9		39.8, C		39.9, C
10	2.43 m	35.7, CH	2.34 m	35.9, CH
11	3.93 dd (10.4, 6.3)	77.8, CH	3.92 t (7.5)	79.1, CH
12	1.74 m	30.2, CH_2	1.80 m	40.5, CH_2
13		47.3, C		47.4, C
14		49.4, C		49.5, C
15	1.21 m	34.1, CH_2	1.16 m	34.2, CH_2
			1.03 m	
16	1.92 dd (13.5, 7.3)	28.0, CH_2	1.92 m	28.3, CH_2
17	1.58 br s	50.3, CH	1.57 m	50.5, CH
18	0.86 s	16.8, CH_3	0.88 s	16.9, CH_3
19	0.94 s	25.9, CH_3	1.09 s	26.0, CH_3
20	1.79 br s	40.9, CH	2.31 m	36.0, CH
21	0.90 d (6.3)	18.6, CH_3	0.92 d (7.6)	18.7, CH_3
22	2.34 m	37.5, CH_2	2.40 m	29.9, CH_2
23	2.59 m	40.3, CH_2	1.36 m	33.3, CH_2
24		215.7, C	3.33 br s	78.9, CH
25	1.55 br s	35.7, CH		73.4, C
26	1.09 s	18.4, CH_3	1.16 s	23.4, CH_3
27	1.09 overlapped	18.5, CH_3	1.21 s	26.8, CH_3
28	1.13 s	25.1, CH_3	1.13 s	25.2, CH_3
29	1.07 s	19.4, CH_3	0.94 s	19.3, CH_3
30	0.82 s	19.2, CH_3	0.82 s	19.4, CH_3

[a] 300 MHz for ^1H and 75 MHz for ^{13}C.

3.5. Cell culture

HepG2 cell line was maintained in MEM supplemented with 10% fetal bovine serum and the cells were grown at 37 °C in an environment of 5% CO_2.

3.6. Western blot analysis

Equal amounts of the whole cell extracts were fractionated by SDS–PAGE and transferred to Hybond-c nitrocellulose membrane (Amersham Bioscience). The membranes were blocked for one hour at room temperature and then incubated overnight at 4 °C in TBST buffer (5% milk) containing related antibody. The membranes were then incubated for an hour at room temperature in TBST buffer (5% milk) containing anti-rabbit IgG or anti-mouse IgG (Jackson-ImmunoResearch, West Grove, PA). Blots were visualized by incubation with SuperSignal West Dura chemiluminescence kit (Pierce Biotechnology) and exposing to light-sensitive film.

3.7. Statistical analysis

All the data were reported as mean ± standard deviation of the mean (SD). Data were analyzed in either one-way ANOVA with an appropriate post hoc test for comparison of multiple groups or unpaired student's test for comparison of two groups as described in figure legends (Graphpad Prism software).

Acknowledgments

This work was supported by the National Natural Science Foundation of China (Grants 90713046, 30925040), and CAS Foundation (Grant KSCX2-YW-R-179).

A. Supplementary data

Supplementary data associated with this article can be found, in the online version, at doi:10.1016/j.bmc.2011.08.030.

References and notes

1. Oh, S.; Kim, S. J.; Hwang, J. H.; Lee, H. Y.; Ryu, M. J.; Park, J.; Kim, S. J.; Jo, Y. S.; Kim, Y. K.; Lee, C. H.; Kweon, K. R.; Shong, M.; Park, S. B. *J. Med. Chem.* **2010**, *53*, 7405.
2. Moller, D. E. *Nature* **2001**, *414*, 821.
3. Hwang, J. T.; Kwon, D. Y.; Yoon, S. H. *New Biotechnol.* **2009**, *26*, 17.
4. Xiao, B.; Heath, R.; Saiu, P.; Leiper, F. C.; Leone, P.; Jing, C.; Walker, P. A.; Haire, L.; Eccleston, J. F.; Davis, C. T.; Martin, S. R.; Carling, D.; Gamblin, S. J. *Nature* **2007**, *449*, 496.
5. The Pharmacopoeia Commission of PRC. *The pharmacopoeia of People's Republic of China*; Chemical Industrial Publishing Press: Beijing, **2005**; Part I, pp 147–148.
6. Kasai, R.; Nie, R. L.; Nashi, K.; Ohtani, K.; Zhou, J.; Tao, G. D.; Tanaka, O. *Agric. Biol. Chem.* **1989**, *53*, 3347.
7. Takasaki, M.; Konoshima, T.; Murata, Y.; Sugiura, M.; Nishino, H.; Tokuda, H.; Matsumoto, K.; Kasai, R.; Yamasaki, K. *Cancer Lett.* **2003**, *198*, 37.
8. Mao, S. L.; Sang, S. M. *Antidiabetic Effect of the Fruit of Siraitia Grosvenori, the Narural Sweetener*. Abstracts of Papers, 239th ACS National Meeting, San Francisco, CA, United States, March 21–25, **2010**.
9. Suzuki, Y. A.; Tomoda, M.; Murata, Y.; Inui, H.; Sugiura, M.; Nakano, Y. *Br. J. Nutr.* **2007**, *97*, 770.
10. Qi, X. Y.; Chen, W. J.; Zhang, L. Q.; Xie, B. *J. Nutr. Res.* **2008**, *28*, 278.
11. Zhang, L. Q.; Qi, X. Y.; Chen, W. J.; Song, Y. F. *Chin. Pharm. Bull.* **2006**, *22*, 237.
12. Qi, X. Y.; Chen, W. J.; Song, Y. F.; Xie, B. *J. Food Sci.* **2003**, *24*, 124.
13. Suzuki, Y. A.; Murata, Y.; Inui, H.; Sugiura, M.; Nakano, Y. *J. Agric. Food Chem.* **2005**, *53*, 2941.
14. Zhou, Y.; Zheng, Y.; Ebersole, J.; Huang, C. F. *Acta Pharm. Sin.* **2009**, *44*, 1252.
15. Murata, Y.; Ogawa, T.; Suzuki, Y. A.; Yoshikawa, S.; Inui, H.; Sugiura, M.; Nakano, Y. *Biosci. Biotechnol. Biochem.* **2010**, *74*, 673.
16. Tan, M. J.; Ye, J. M.; Turner, N.; Cordula, H. B.; Ke, C. Q.; Tang, C. P.; Chen, T.; Weiss, H. C.; Gesing, E. R.; Rowland, A.; James, D. E.; Ye, Y. *Chem. Biol.* **2008**, *15*, 263.
17. Takemoto, T.; Arihara, S.; Nakajima, T.; Okuhira, M. *Yakugaku Zasshi* **1983**, *103*, 1155.
18. Tunmann, P.; Stapel, G. *Arch. Pham.* **1966**, *299*, 579.
19. Qi, C.; Chen, D. H.; Si, J. Y.; Shen, L. G. *Bopuxue Zazhi* **1994**, *11*, 43.
20. Brusq, J. M.; Ancellin, N.; Grondin, P.; Guillard, R.; Martin, S.; Saintillan, Y.; Issandou, M. *J. Lipid Res.* **2006**, *47*, 1281.